Cancer Research Journal
2025, Vol. 13, No. 1, pp. 9-22
https://doi.org/10.11648/j.crj.20251301.12

Research Article

A Novel Ferroptosis-Related lncRNA Prognostic Signature for Colorectal Cancer by Bioinformatics Analysis

Yujiao Zhang[1, †], Guodong Yang[2, †], Jiping Wang[3], Huaxin Duan[4, *]

[1]Respiratory Medicine, Huanggang Central Hospital Affiliated to Yangtze University, Huanggang, China
[2]Department of Oncology, Huanggang Central Hospital Affiliated to Yangtze University, Huanggang, China
[3]Department of Radiotherapy, Huanggang Central Hospital Affiliated to Yangtze University, Huanggang, China
[4]Department of Oncology, Hunan Provincial People's Hospital, Changsha, China

Abstract

Recently, extensive studies have shown that ferroptosis boosted a perspective for its usage in cancer therapeutics. The current study aims to construct a robust ferroptosis-related lncRNAs signature prediction model to increase the predicted value of colorectal cancer (CRC) by bioinformatics analysis. By comparing CRC tissue with adjacent normal tissues, we screened 2541 differentially expressed lncRNAs from The Cancer Genome Atlas (TCGA) CRC using the R language and "limma" package, of which 439 are ferroptosis-related lncRNAs. Univariate Cox regression, lasso regression, multivariate Cox regression are used to construct a seven ferroptosis-related lncRNAs (AC005550.2, LINC02381, AL137782.1, C2orf27A, AC156455.1, AL354993.2, AC008760.1) prognostic signature in train set. This model's prognosis in the high-risk group is worse than that of the low-risk group in the train set, test set, and entire set. Based on the stratification of clinical variables (gender, age, clinical stage, postoperative tumor status, CEA levels, perineural invasion, vascular invasion, mismatch repair (MMR) and gene mutation status (KRAS, BRAF)), the high-risk group's prognosis is also worse than that of the low-risk group. The area under curve (AUC) of receiver operating characteristic (ROC) curve for predicting three years survival in the train set, test set, and entire set were 0.796, 0.715, and 0.758, respectively. Furthermore, Univariate Cox regression and multivariate Cox regression displayed that the signature could serve as an independent prognostic factor; meanwhile, we draw the nomogram based on multivariate Cox regression ($P<0.05$). Compared to clinical variables, this signature's ROC curves demonstrated the second largest AUC value (0.737). The expression of these lncRNAs and the lncRNA signature are related to clinical stage, T stage, Lymph-node status, distant metastasis, KRAS mutation, BRAF mutation, MMR status, and perineural invasion. Finally, GSEA analysis results show that the signature is involved in six KEGG signal pathways, such as KEGG_HEDGEHOG_SIGNALING_PATHWAY, KEGG_ALPHA_LINOLENIC_ACID_METABOLISM, KEGG_ARACHIDONIC_ACID_METABOLISM, KEGG_CITRATE_CYCLE_TCA_CYCLE, KEGG_PENTOSE_PHOSPHATE_PATHWAY, KEGG_FRUCTOSE_AND_MANNOSE_METABOLISM. In conclusion, the current study shows a seven ferroptosis-related lncRNA signature could efficiently function as a novel and independent prognosis biomarker and therapeutic target for CRC patients.

[*]Corresponding author: 317102912@qq.com (Huaxin Duan)

† Yujiao Zhang and Guodong Yang are co-first authors.

Received: 3 April 2025; **Accepted:** 21 April 2025; **Published:** 19 May 2025

Keywords

lncRNA, TCGA, Ferroptosis, Colorectal Cancer, Signature

1. Introduction

It is estimated that there will be more than 1.8 million new cases of colorectal cancer (CRC) and 881,000 deaths in 2018, accounting for approximately one in 10 cancer cases and deaths. Overall, colorectal cancer ranks third in incidence but second in mortality [1]. Despite the fact that recent advances in the genetic and molecular characterization of tumors and the 5-year survival rate of early CRC was more than 90%, the 5-year survival rate of metastatic colorectal cancer was less than 14%, and the prognosis was very poor [2]. Therefore, investigating promising prognostic signatures along with potential targets is considered as an essential phase to achieving this goal.

Ferroptosis is an oxidative, iron-dependent form of cell death that is distinct from apoptosis, classic necrosis, ferroptosis, and other forms of cell death, which is triggered by inactivation of cellular glutathione (GSH)-dependent antioxidant defenses, leading to the accumulation of toxic lipid ROS (L-ROS) [3, 4]. Recent studies have shown that ferroptosis plays an important regulatory role in the occurrence and development of many diseases, such as tumors, nervous system diseases, ischemia-reperfusion injury, kidney injury, and blood diseases, and has become the focus and hotspot of research on the treatment and prognosis improvement of related diseases [5]. Mostly, ferroptosis is gradually accepted as an adaptive feature to eliminate the malignant cells and plays a pivotal role in the depression of tumorigenesis by removing the cells that are deficient in key nutrients in the environment or damaged by infection or ambient stress [6]. Previous studies have reported that some inducers, such as RSL3 [7], β-elemene [8], Resibufogenin [9], andrographis [10], bromelain [11], IMCA [12], talaroconvolutin A (TalaA) [13], ACADSB [14], erastin [15], dichloroacetate [16], B. etnensis Raf. extract [17], circABCB10 [18] suppressed the progression of CRC via inducing ferroptosis. Hence, it is essential to discover ferroptosis-linked biomarkers that can be applied as valuable early diagnostic as well as prognostic biomarkers for CRC patients.

Long non-coding RNAs (lncRNAs), a class of non-coding RNAs, which are more than 200 nucleotides long, have apparently little or no protein-coding ability [19]. LncRNAs regulate critical biological functions related to cell growth and survival, genomic imprinting, chromatin modifications, and allosteric regulation of enzyme activities [20]. Besides, a mounting number of studies have chronicled that lncRNAs affect cancer progression and predict dismal prognosis in diverse cancer types by modulating ferroptosis. For example, p53 related lncRNA (P53RRA) promotes ferroptosis and apoptosis in cancer by activating the p53 pathway [21]. LncRNA GABPB1-AS1 regulates oxidative stress during erastin-induced ferroptosis in HepG2 hepatocellular carcinoma cells [22]. LncRNA-linc00336 inhibits ferroptosis in lung cancer by functioning as a competing endogenous RNA [23]. Linc00618 accelerates ferroptosis via inhabiting vincristine (VCR) and lymphoid-specific helicase (LSH) /SLC7A11 in leukemia [24]. LncRNA-MT1DP loaded by folate-modified liposomes sensitizes erastin-induced ferroptosis via regulating miR-365a-3p/NRF2 axis in non-small cell lung cancer cells [25]. Hence, it is critical to explore the pivotal lncRNAs closely linked to ferroptosis along with prognosis in CRC.

This study is the first to propose a predictive model of lncRNA related to ferroptosis genes in tumors. Therefore, we postulated that ferroptosis-linked lncRNAs could be valuable prognostic biomarkers for CRC patients. Herein, we explored the expression of lncRNAs in CRC from The Cancer Genome Atlas (TCGA) and identified ferroptosis -associated lncRNAs with prognostic potential. We constructed and verified a seven ferroptosis-correlated lncRNA biosignature with the ability to estimate the survival prognosis of CRC patients.

2. Materials and Methods

2.1. Data Download and Processing

The transcriptome data (Cases (544): Primary Site (colon and rectum), Program (TCGA), Project (TCGA-COAD and TCGA-READ); Files (612 including 568 CRC tissues and 44 non-CRC tissues): Data Category (Transcriptome Profiling), Workflow Type (HTSeq - FPKM)), Data Type (Gene Expression Quantification), clinical information (Files (548), Data Category (clinical), and Data Format (bcr xml)) were abstracted from The Cancer Genome Atlas (TCGA) web data resource (https://cancergenome.nih.gov/) on November 20, 2020 (Table 1). Patients with no follow-up time and follow-up time shorter than 30 days were excluded from this study.

Table 1. *Summary of patient cohort information for CRC.*

Clinical variables	Case	Percentage
Gender		

Clinical variables	Case	Percentage
Male	242	46.36%
Female	280	53.64%
Age (years)		
Range	33-88	
Median	66	
Race		
ASIAN	8	1.53%
BLACK	53	10.15%
AMERICAN INDIAN	1	0.19%
WHITE	393	75.29%
unknow	67	12.84%
Clinical Stage		
Stage I	279	53.45%
Stage II	124	23.75%
Stage III	85	16.28%
Stage IV	26	4.98%
unknow	8	1.53%
T stage		
T1+Tis	172	32.95%
T2	281	53.83%
T3	47	9.00%
T4	19	3.64%
Tx	3	0.57%
Lymph node status		
N0	335	64.18%
N1	98	18.77%
N2	75	14.37%
N3	2	0.38%
Nx+unknow	12	2.30%
Metastasis		
M0	353	67.62%
M1	25	4.79%
Mx+unknow	144	27.59%
Eml4-Alk translocation status		
Yes	34	6.51%
No	213	40.80%
unknow	275	52.68%
EGFR mutation status		
Yes	80	15.33%
NO	197	37.74%
unknow	285	54.60%
KRAS mutation status		
Yes	62	11.88%
No	253	48.47%
unknow	207	39.66%
Postoperative tumor status		
WITH TUMOR	111	21.26%
TUMOR FREE	314	60.15%
unknow	97	18.58%
History neoadjuvant treatment		
Yes	3	0.57%
No	518	99.23%
unknow	1	0.19%

2.2. Screening of Ferroptosis-related lncRNAs (FRlncRNAs)

The ferroptosis genes (259) were downloaded from the world's first database of ferroptosis regulators and markers and ferroptosis-disease associations (FerrDb) (http://www.zhounan.org/ferrdb/). We employed the "limma" R package [26] to screen differentially expressed lncRNAs by comparing 568 CRC tissues with 44 adjacent non-CRC tissues. The included criteria are False Discovery Rate (FDR) < 0.05 and |logFC|>1. Furthermore, we identified ferroptosis-related lncRNAs by the correlation analysis between the lncRNAs expression levels and the ferroptosis genes based on the criteria of $P < 0.001$and |Correlation Coefficient| > 0.3.

2.3. Development, Verification, and Assessment of Prognostic Biosignature

We utilized the R language 4.0.1version "caret" package to randomly classify the entire data set (Supplement Table 1) with FRlncRNAs expression profiles into two sets (train set (Supplement Table 2) and test set (Supplement Table 3), and conducted univariate Cox regression for FRlncRNAs in the train group ($P<0.05$). Lasso regression was used to avoid overfitting by "glmnet" package [27] ($P<0.05$). Afterward, multivariate Cox regression was employed to develop the optimal prognostic risk model and took advantage of the function of "coxph" and "direction=both" via the R language "survival" package [28] ($P<0.05$). Then, the prognostic lncRNA signature's risk score constituting multiple lncRNAs was developed on the basis of the summation of the product of each lncRNA and its coefficient. Additionally, the Propor-

tional Hazards Assumption was tested in the Cox model. Similarly, on the basis of the previous training set's risk score formula, we applied it to the testing set as well as the entire set as validation.

This model was employed to explore each patient's survival prognosis by the Kaplan-Meier curve along with the log-rank test on the basis of the median of risk score, namely high-risk group and low-risk group in the train set, test set, entire set. The lncRNA signature's predictive power was explored by computing the AUC of three years dependent ROC curve by the "survival ROC" package [29].

To further enhance the prognostic signature's credibility, we conducted a stratified survival prognostic analysis on gender, age, clinical stage, postoperative tumor status, CEA levels, perineural invasion, vascular invasion, mismatch repair (MMR) and gene mutation status (KRAS, BRAF).

2.4. Independent and Prognostic Ability of the lncRNA Signature

The univariate Cox regression and multivariate Cox regression were utilized to analyze the independent and prognostic ability of the lncRNA signature in the train set (Supplement Table 4), test set (Supplement Table 5), and entire set (Supplement Table 6). The clinical parameters include age, gender, clinical stage, T stage, lymph nodes as well as distant metastasis. Besides, compared with clinical variables, The ROC curve was employed to explore whether the lncRNA biosignature has better predictive power. The "rms" package was employed to construct the nomogram according to the multivariate Cox regression result (P<0.05). To further investigate whether the ferroptosis -associated lncRNAs are involved in CRC development, we explored the relationship of the ferroptosis-linked lncRNAs' expression with clinical variables using the Kruskal-Wallis test and Wilcoxon rank-sum test.

2.5. GSEA Analysis of the lncRNA Signature

Gene set enrichment analysis (GSEA4.1.0) downloaded from https://www.gsea-msigdb.org/gsea/index.jsp website was used to identify the biological function of the prediction model [30]. Based on the median expression of lncRNA signature riskScore in 568 tumor samples, we divided them into high and low-risk groups for KEGG analysis of GSEA. The abundant signaling cascades in each phenotype were based on the nominal (NOM) P-value, the normalized enrichment score (NES), as well as the false discovery rate (FDR). FDR < 25% and NOM P-value < 5% serve as a standard for inclusion.

2.6. Statistical Analysis

R software 4.0.3 version and attached packages were employed to perform statistical analyses. All the statistical tests were two-sided. P <0.05 signified of statistical significance.

3. Results

3.1. Screening of Ferroptosis-related lncRNAs in CRC

Comparing CRC tissues with adjacent non-CRC tissues, there are a total of 2541 differentially expressed lncRNAs, of which 1805 are up-regulated and 736 are down-regulated (Supplement Table 7). The correlation results between 259 ferroptosis-related genes and differentially expressed lncRNAs shown that there are 439 ferroptosis-related lncRNAs (FRlncRNAs) (Supplement Table 8).

3.2. Construction, Validation, and Evaluation of a Seven Ferroptosis-related lncRNAs Prognostic Signature

The entire set (N=506) with 439 FRlncRNAs expression profiles was grouped randomly into the train set (N=254) and test set (N=252). The univariate Cox regression assessment displayed that a total of 22 lncRNAs were linked to the overall survival of the patients in the train set (Figure 1A). Lasso regression was used for further analysis to eliminate overfitting lncRNAs, and the 16 lncRNAs we obtained were used for the subsequent multivariate Cox regression analysis (Figure 1B-1C) (concordance index [C-index], 0.75). The ferroptosis-associated lncRNA prognostic biosignature was developed based on the summation of the product of each lncRNA expression and its coefficient in multivariate Cox regression as indicated below: lncRNA biosignature risk score= (0.136× expression of AC005550.2) + (0.240× expression of LINC02381) + (-1.407× expression of AL137782.1) + (0.365× expression of C2orf27A) + (0.235× expression of AC156455.1) + (0.280× expression of AL354993.2 1) + (0.653× expression of AC008760.1). Besides, the results testing the Proportional Hazards Assumption in the Cox model revealed that all the P values were greater than 0.05, implying they meet the PH test (Supplement Table 9).

According to the median value of the risk score, the Kaplan-Meier curves demonstrate that the high-risk group has a remarkably dismal overall survival (OS) in contrast with the low-risk group in the train set (P=2.899E-06), test set (P=5.314E-03), and entire set (P=1.1E-06) (Figure 2A-C). The train set shows three years' OS for patients with high and low-risk group were 60.6% and 90.5%, respectively. The test set is 63.9% and 90.1%, respectively. The entire set is 60.6% and 90.5%, respectively. The AUC of three years dependent ROC for the seven-lncRNA biosignature achieves 0.796, 0.715, and 0.758 respectively in the train set, test set, and entire set (Figure 2D-F), which demonstrate the good performance of the model in estimating the CRC patients' OS. The patients with high-risk scores have higher mortality relative to those with low-risk scores in the three sets (Figure 2 H-J). The six lnRNAs' (AC005550.2, LINC02381, C2orf27A,

AC156455.1, AL354993.2, AC008760.1) expression of signature were higher in high-risk group than that in low-risk group, AL137782.1 oppositely (Figure 2 K-M).

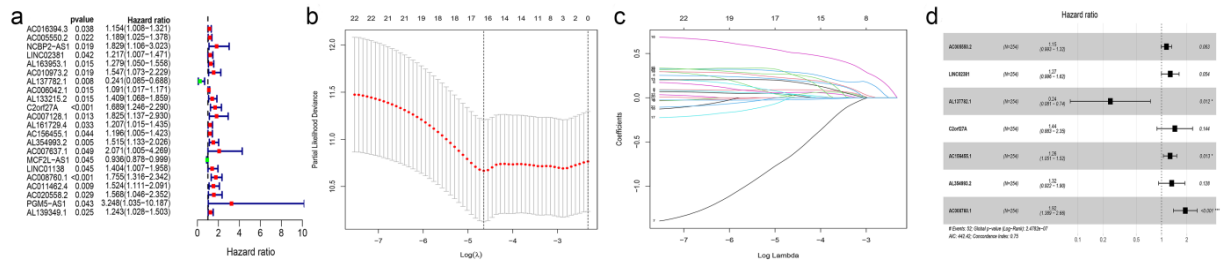

Figure 1. *Construction of the ferroptosis-related lncRNAs prognostic signature. Univariate Cox regression (A), Lasso regression (B-C), Multivariate Cox regression (D).*

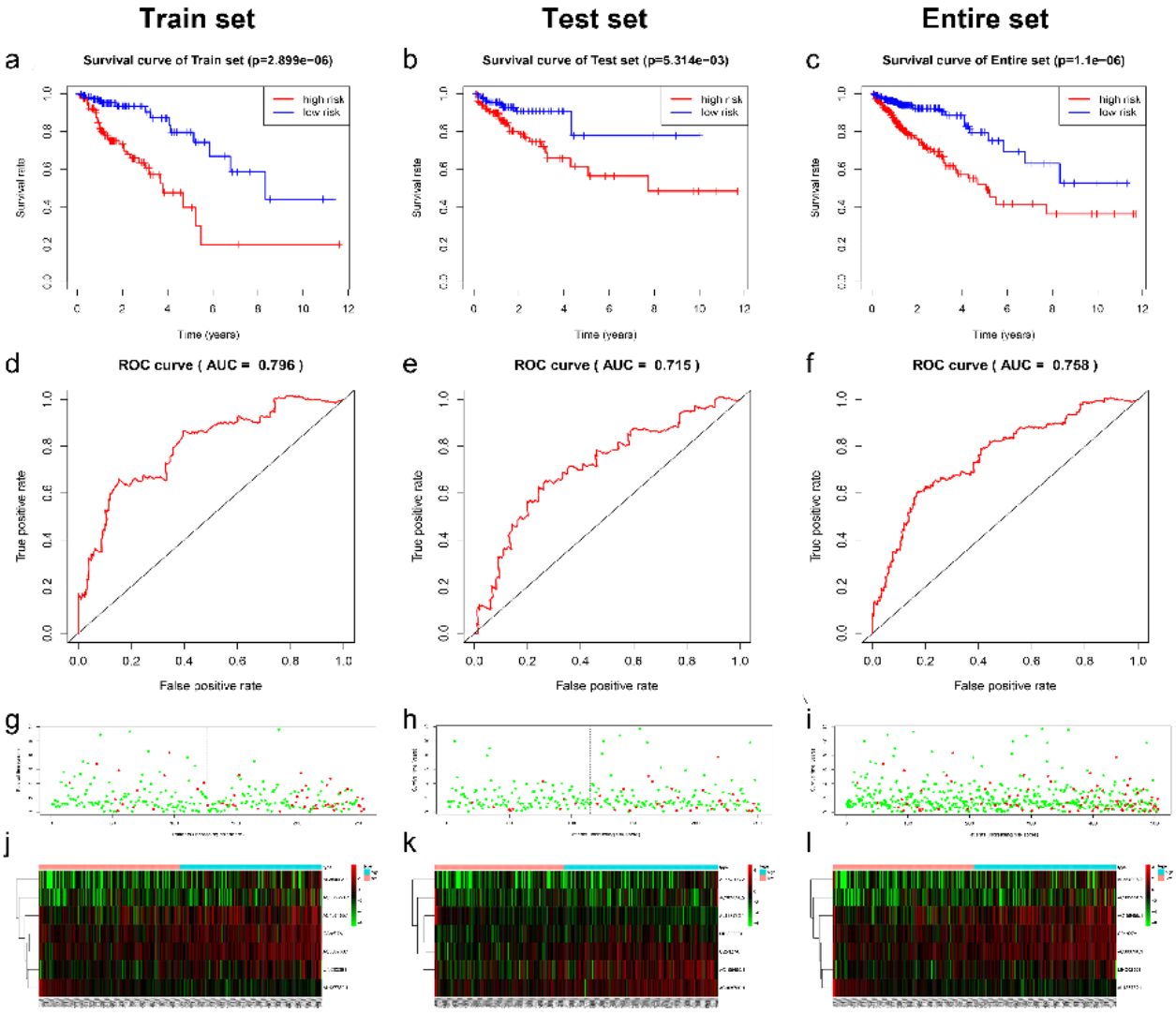

Figure 2. *Validation and evaluation of the ferroptosis-related lncRNAs prognostic signature. Kaplan-Meier curves in the train set (A), test set (B), entire set (C); The AUC of three years dependent curve in the train set (D), test set (E), entire set (F); Survival status in high and low-risk patients for train set (G), test set (H), entire set (I), red dots represent death, and green dots represent alive; The cluster heat map of seven lncRNAs' expression in high and low risk groups for the train set (J), test set (K), entire set (L).*

It is worth noting that AC156455.1, and AL354993.2's high expression of this lncRNA signature also has a worse OS than

low (Figure 3). The relationship between these seven lncRNAs and ferroptosis genes is shown in Figure 4. In addition, we stratified according to various clinical factors (clinical stage, gender, age, CEA levels, MMR status, postoperative tumor status, perineural invasion, vascular invasion, KRAS mutation, BRAF mutation) and applied the prognostic model to OS detection, which is shown in Figure 5, the results shown that the signature has good predictive significance for CRC patients in most stratification factors, and part of results are not satisfactory (P>0.05), which might be due to there are not enough samples in these stratification.

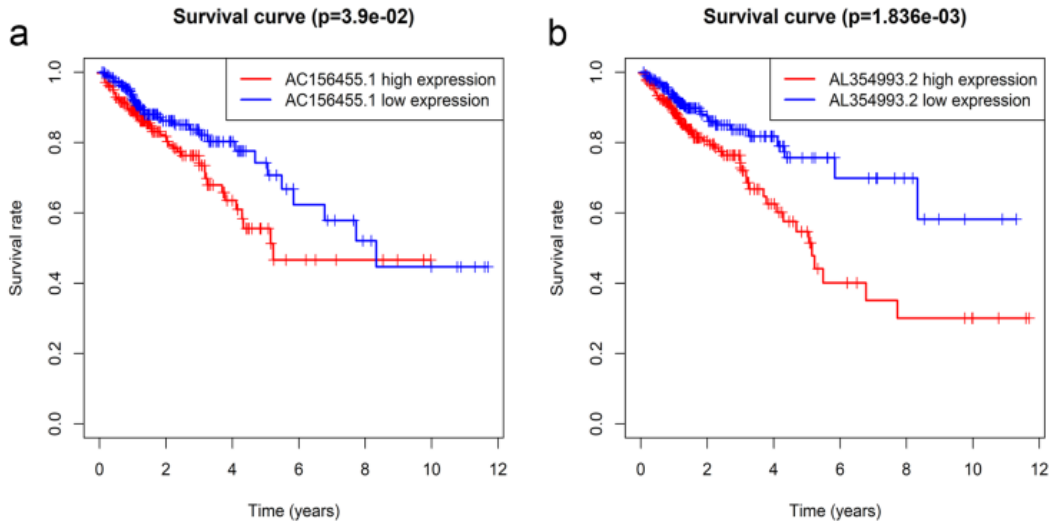

Figure 3. *Two lncRNAs associated with overall survival in CRC patients using Kaplan–Meier curves and log-rank tests. The patients were stratified into high and low expression groups based on the median expression of each lncRNA. (A) AC026355.1. (B) AC099850.3.*

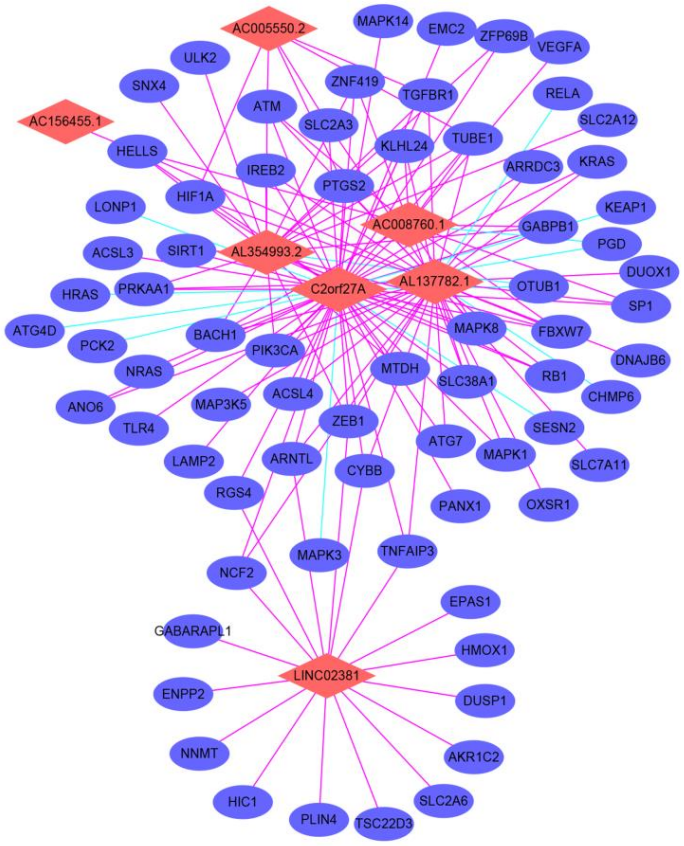

Figure 4. *The network relationship between the seven lncRNAs and ferroptosis genes. Prismatic represent lncRNA, and oval represent ferroptosis genes. The red line represents positive correlation, and blue represents negative correlation.*

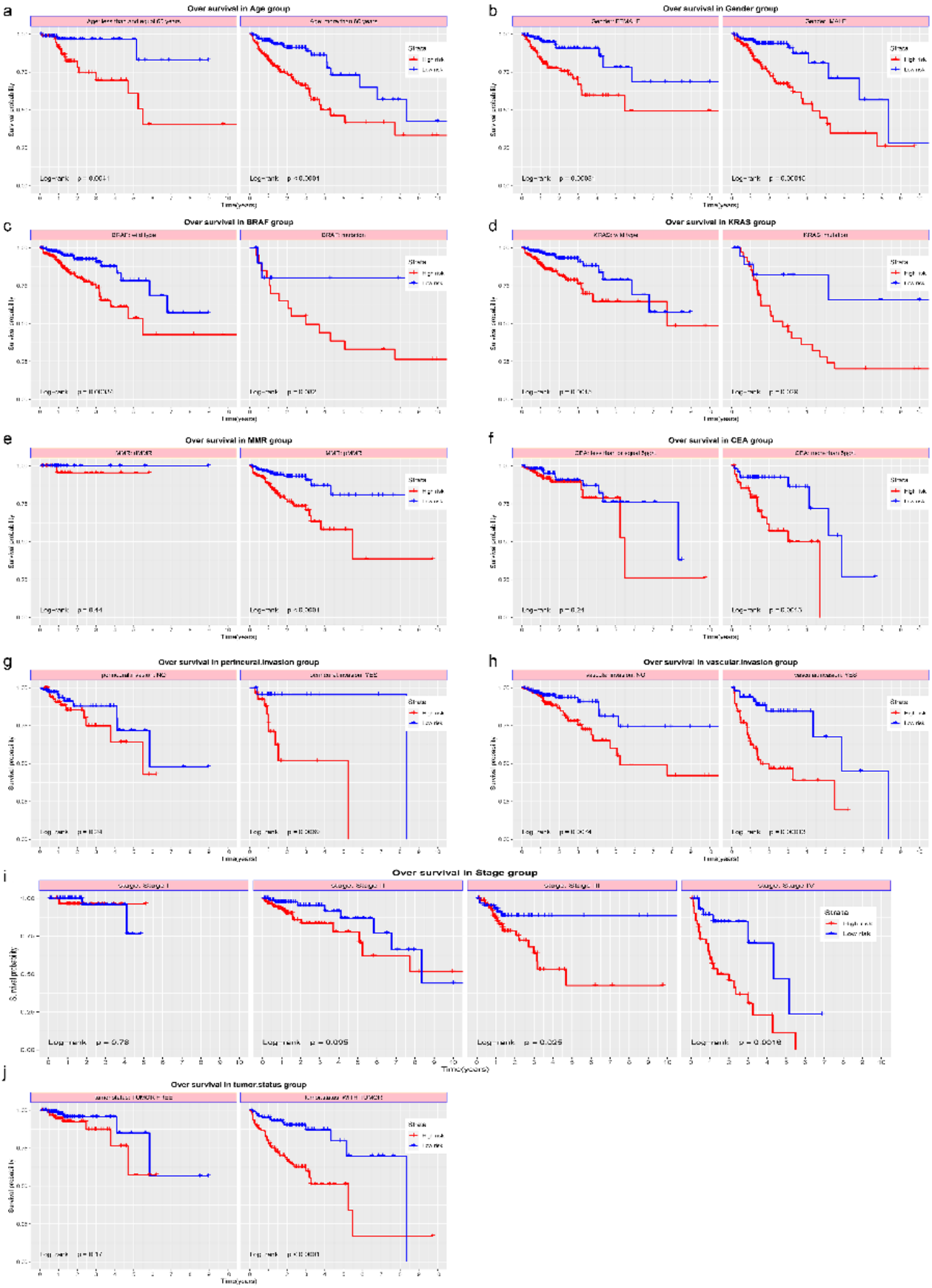

Figure 5. *The overall survival of the ferroptosis-related lncRNAs prognostic signature in the stratification of clinical variables. Gender group (A), Age group (B), Stage group (C), KRAS group (D), BRAF group (E), MMR group (F), CEA group (G), Perineural invasion group (H), Vascular invasion group (I), Tumor status group (J).*

3.3. Independent Prognostic Analysis of the Seven Ferroptosis-associated lncRNAs Signature and Its Correlation with Clinical Variables

The Univariate Cox regression assessment demonstrated that the lncRNA biosignature risk score was evidently correlated with the patients' OS (hazard ratio HR=1.224, confidence interval 95%CI=1.149–1.303, P=3.69E-10) in train set, (HR=1.160, 95%CI=1.016–1.325, P=0.028) test set, and (HR=1.179, 95%CI=1.125–1.235, P=7.04E-12) entire set (Table 2). Moreover, the multivariate Cox regression analysis showed that the lncRNA biosignature risk score remained independent with OS considering other conventional clinical factors including Lymph-node status, the clinical stage, distant metastasis, and T stage (HR=1.187, 95% CI=1.107–1.273, P=1.39E-06) in the train set, and (HR=1.122, 95% CI=1.067–1.180, P=8.33E-06) in entire set, in spite of P>0.05 (HR=1.059, 95% CI=0.995–1.289, P=0.059) in test set. Meanwhile, T stage and age were demonstrated as an independent prognostic index. Compared to clinical variables, this signature risk score's ROC curves of three years demonstrate the second-largest AUC value (0.737) (Figure 6A). On the basis of the multivariate Cox regression results, we constructed the nomogram of the clinical prediction model (C-index, 0.781) (Figure 6B).

Table 2. *Univariate and multivariate Cox regression of clinical features.*

Clinical features	univariate Cox regression				multivariate Cox regression			
	HR	HR.95L	HR.95H	pvalue	HR	HR.95L	HR.95H	pvalue
Age (continuous variable)	0.997	0.978	1.015	0.718	1.003	0.984	1.023	0.738
Gender	1.000	0.694	1.441	1.000	1.213	0.828	1.775	0.322
Clinical stage	1.648	1.396	1.946	0.000	1.985	1.241	3.175	0.004
T stage	1.600	1.285	1.994	0.000	1.155	0.909	1.468	0.237
Distant metastasis	1.748	0.959	3.187	0.068	0.395	0.118	1.319	0.131
Lymph-node status	1.787	1.455	2.195	0.000	0.992	0.665	1.481	0.970
An eight ferroptosis-related lncRNAs signature	1.039	1.022	1.058	0.000	1.040	1.020	1.061	0.000

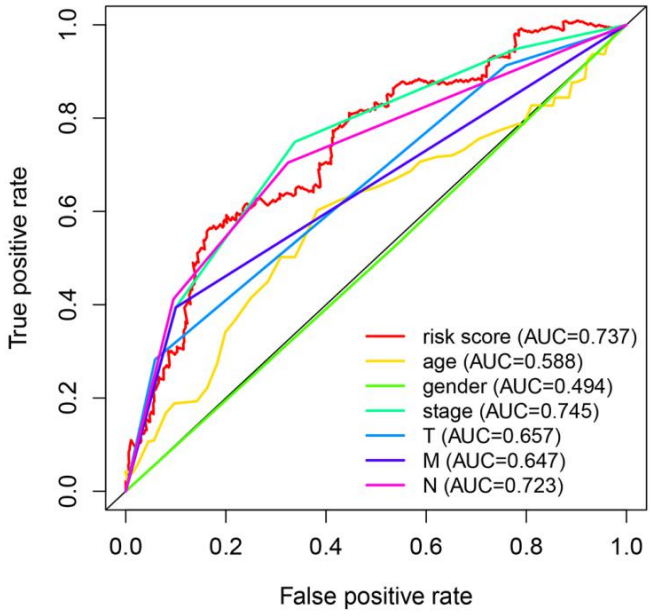

Figure 6. *The ROC curve and nomogram of the ferroptosis-related lncRNAs prognostic signature. ROC curve compared to clinical variables (A), Nomogram (B).*

Based on the stratification of clinical variables, the correlation between the lncRNAs and clinical variables shows that LINC02381' expression is related to T stage, Lymph-node status, and clinical stage, KRAS mutation, BRAF mutation, and perineural invasion. C2orf27A' expression is associated with T stage, Lymph-node status, clinical stage, KRAS mutation, MMR. AC156455.1' expression is correlated to Lymph-node status. AL354993.2' expression is connected to Lymph-node status, distant metastasis, clinical stage, KRAS mutation. AC008760.1' expression is concerning to Lymph-node status, distant metastasis, clinical stage, KRAS mutation. AL137782.1' expression is linked to KRAS mutation. The lncRNA signature' riskscore is coupled to T stage, Lymph-node status, distant metastasis, clinical stage, and KRAS mutation. (Figure 7).

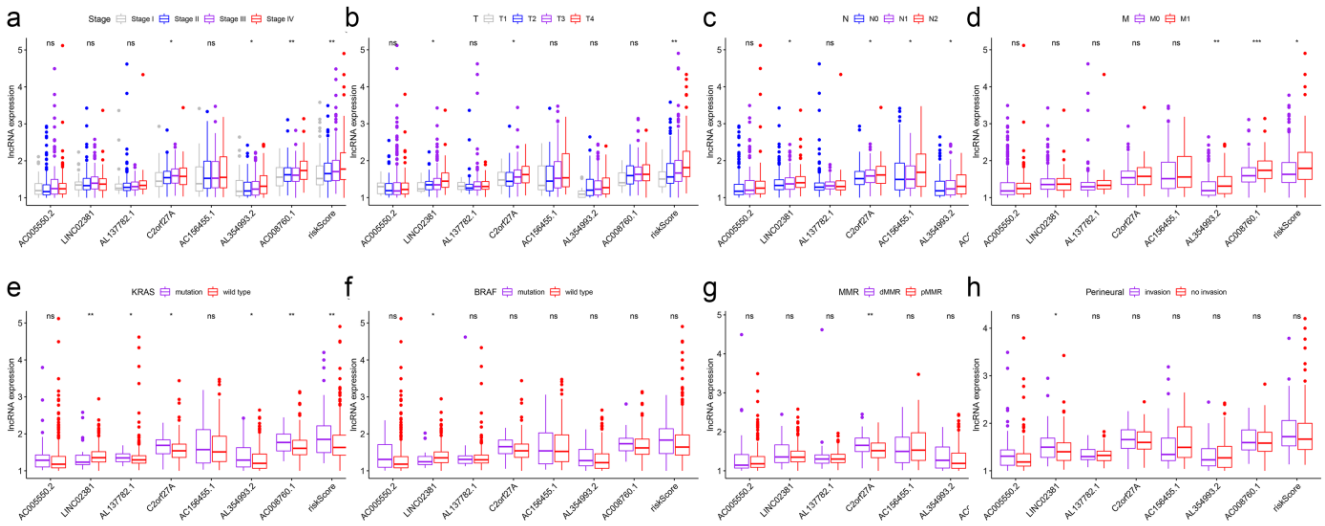

Figure 7. *The correlation between the lncRNAs constituting the signature and clinical variables. Clinical stage (A), T stage (B), Lymph-node status (C), Distant metastasis (D), EGFR status (E), Eml4-Alk translocation status (F), KRAS status (G). * represents P<0.05, ** represents P<0.01, *** represents P<0.001, "ns" represents no statistical significance.*

3.4. Functional Enrichment Analysis of the Seven Ferroptosis-related lncRNAs Signature

GSEA analysis is used to discover potential biological functions of the seven ferroptosis-associated lncRNAs signature of CRC (Figure 8). The results showed that three signaling pathways (KEGG_HEDGEHOG_SIGNALING_PATHWAY, KEGG_ALPHA_LINOLENIC_ACID_METABOLISM, KEGG_ARACHIDONIC_ACID_METABOLISM) are obviously enriched in the high-risk group, and three signaling cascades (KEGG_CITRATE_CYCLE_TCA_CYCLE, KEGG_PENTOSE_PHOSPHATE_PATHWAY, KEGG_FRUCTOSE_AND_MANNOSE_METABOLISM) were abundant in the low-risk group by c2.cp.kegg.v7.2.symbols.gmt. These results suggest that this signature model may influence CRC progression and prognosis mainly through metabolism-related pathways.

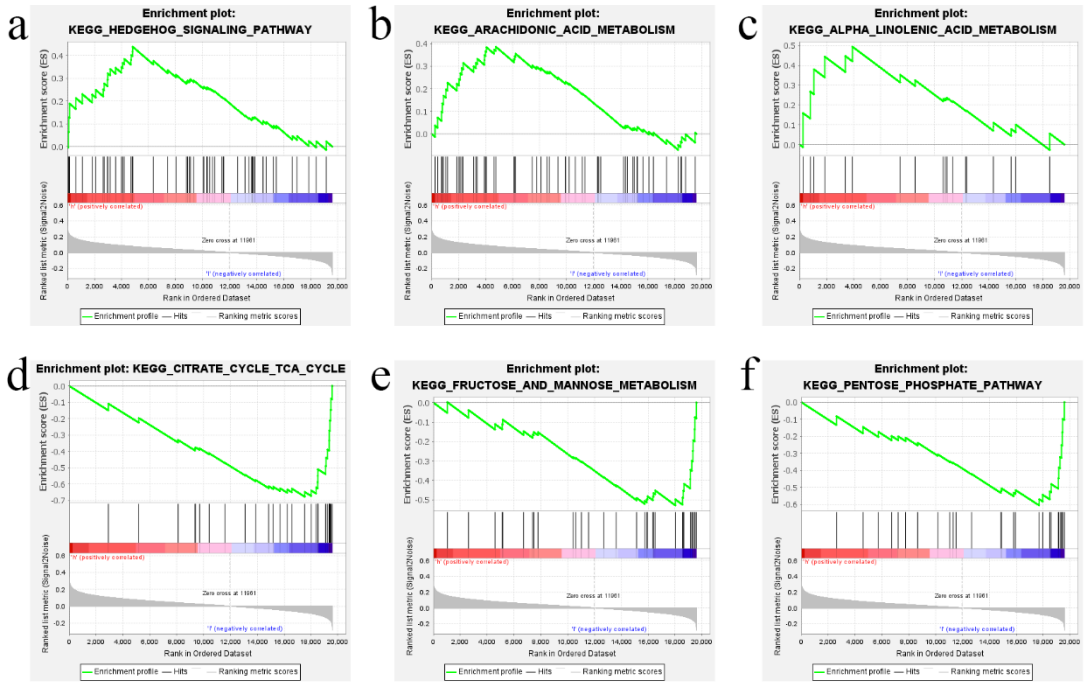

Figure 8. *The KEGG enrichment analysis of GSEA enriched in the high-risk group and low-risk group of the ferroptosis-related lncRNAs prognostic signature.* KEGG_HEDGEHOG_SIGNALING_PATHWAY(A), KEGG_ARACHIDONIC_ACID_METABOLISM(B), KEGG_ALPHA_LINOLENIC_ACID_METABOLISM (C), KEGG_CITRATE_CYCLE_TCA_CYCLE (D). *KEGG_FRUCTOSE_AND_MANNOSE_METABOLISM(E), KEGG_PENTOSE_PHOSPHATE_PATHWAY(F)).*

4. Discussion

CRC is a highly common malignant carcinoma, which is particularly prone to liver and lung metastasis, seriously affecting the survival prognosis of patients [31]. Therefore, finding a prognostic marker with high specificity and sensitivity is becoming more and more urgent for patients. Although the current treatment methods have made great advancements, the prognosis is still very poor. Ferroptosis is a recently recognized cell death modality that is morphologically, biochemically and genetically distinct from other forms of cell death and that has emerged to play an important role in cancer biology [3]. In addition, extensive studies have documented that lncRNA plays a very important role in regulating gene expression and regulation in tumor [20, 32]. However, there are few reports on lncRNA regulating ferroptosis in tumors. Although two previous genetic prognostic models of ferroptosis have been reported in hepatocellular carcinoma [33] and glioma [34], our study is the first to report the study of ferroptosis-related lncRNA prognostic models in tumors.

In the present study, we downloaded ferroptosis genes from FerrDb, and used the R language and its attached packages to find differentially expressed lncRNAs related to ferroptosis (FRlncRNAs). We randomly grouped all the patients into train set as well as the test set, then a seven ferroptosis-related lncRNAs signature model (AC005550.2, LINC02381, AL137782.1, C2orf27A, AC156455.1, AL354993.2, AC008760.1) was established through univariate Cox regression, Lasso regression, as well as multivariate Cox regression in the train set. At the same time, the biosignature was verified in the test set as well as the entire set. On the basis of the median risk score, the Kaplan-Meier curves revealed that the high-risk group had an evidently dismal overall survival relative to the low-risk group in the three data sets and various clinical stratification factors. Assessment of the biosignature for OS in the three sets by ROC curve exhibited well predictive value. The Univariate Cox regression as well as the multivariate Cox regression analyses demonstrated that the biosignature had independent prognostic ability considering other conventional clinical variables for CRC patients. On the basis of the multivariate Cox regression results, we developed the nomogram of the clinical prediction model. Furthermore, the seven lncRNAs and the signature model are linked to the T stage, Lymph-node status, distant metastasis, clinical stage, KRAS mutation, BRAF mutation, and perineural invasion to varying degrees. Finally, GSEA analysis results show that the signature model is involved in six KEGG signal pathways based on high and low-risk group, such as KEGG_HEDGEHOG_SIGNALING_PATHWAY, KEGG_ALPHA_LINOLENIC_ACID_METABOLISM, KEGG_ARACHIDONIC_ACID_METABOLISM, KEGG_CITRATE_CYCLE_TCA_CYCLE, KEGG_PENTOSE_PHOSPHATE_PATHWAY, KEGG_FRUCTOSE_AND_MANNOSE_METABOLISM. These results suggest that this signature model may influence CRC progression and prognosis mainly through metabolism-related pathways.

Before this study, many prognostic models of CRC have been constructed from different research perspectives. For example+, Yang G et al. identified a five-microRNA signature as prognostic biomarker in CRC by bioinformatics analysis [35]. Bai J et al. developed a novel 14-gene immune-related signature that may potentially serve as a prognostic predictor for CRC [36]. Zhang J et al. screened gene signature of prognostic m6A modulators in CRC [37]. Xiao G et al. constructed a risk signature with inflammatory and t immune cells infiltration in CRC predicting distant metastases and efficiency of chemotherapy [38]. Tokunaga R et al. presented a 12-chemokine signature, a predictor of tumor recurrence in colorectal cancer [39]. Zong Z et al. demonstrated a prognostic alternative splicing signature by differential splicing patterns of 13 genes in CRC [40]. Li K et al. revealed a six gene-specific DNA methylation signature for CRC [41]. Zhou Z et al. developed and validated of an autophagy signature based on 5 autophagy genes for the prediction of post-operative survival in CRC [42]. Wu B et al. developed an immune infiltration-related eight-gene prognostic signature in CRC microenvironment [43]. These examples are only the tip of the iceberg. At present, there are no reports about the prognostic model of lncRNA related to ferroptosis in tumors.

Among these lncRNAs of the signature, some studies have shown that LINC02381 is related to immune gene [44] and autophagy gene [45] in colon adenocarcinoma. LINC02381 might suppress human CRC tumorigenesis partly by regulating PI3K signaling pathway [46]. LINC02381 inhibits gastric cancer progression and metastasis through regulating wnt signaling pathway [47]. However, LINC02381 functions as a cancer-promoting gene to promote cell viability and migration via targeting mir-133b / RhoA in cervical cancer cells [48]. AC008760.1 was reported to be related to autophagy, and Li et al. constructed a autophagy-related lncRNA prognosis model in CRC [49]. The remaining lncRNAs have not seen relevant reports in previous studies.

Our study found that the expression of these lncRNAs and the constructed prognostic signature were closely related to the patient's clinical stage, T stage, Lymph-node status, distant metastasis, KRAS mutation, BRAF mutation, MMR status and perineural invasion, especially the KRAS mutation, BRAF mutation and MMR status. These features have an important guiding significance for patients' medication. So can we explore whether these lncRNAs regulate these variables and how to regulate them? There have been many studies about ferroptosis in the drug resistance of tumor patients [50, 51]. The current study demonstrated the prognostic significance of these ferroptosis-related lncRNAs and signature in CRC. Therefore, we have reason to believe that these lncRNAs are worthy of in-depth research in tumor resistance mechanisms.

Our current study also has some limitations. First, we use the data in the TCGA database as the starting point for research; although the model has been internally verified, it is still needed for further verification in external data; second, TCGA's race is mainly white (75%), and whether the model fits other race needs further verification. Third, the analysis of the lncRNA expression of the model and the KEGG function enrichment analysis by the GSEA model requires further cell function experimental analysis.

5. Conclusion

Herein, we established a novel ferroptosis-related lncRNA prognostic signature model comprising seven lncRNAs (AC005550.2, LINC02381, AL137782.1, C2orf27A, AC156455.1, AL354993.2, AC008760.1) in CRC. In the future, the seven ferroptosis-related lncRNA prognostic biosignature could enhance predictive accuracy as well as guide individualized therapy for CRC patients with prospective validation. Future studies should include in vitro/in vivo functional experiments (e.g., CRISPR knockout of the identified lncRNAs AC005550.2 and LINC02381) to validate their mechanistic roles in ferroptosis regulation and CRC progression. Prospective multicenter clinical trials are needed to evaluate the signature's predictive accuracy in diverse ethnic populations, particularly given the TCGA cohort's Caucasian predominance (75%). Standardized assays for lncRNA detection in liquid biopsies should be developed for clinical application. Further investigations should explore how these lncRNAs interact with ferroptosis drivers (e.g., GPX4, SLC7A11) through ceRNA networks or epigenetic modifications, using techniques like RIP-seq and ChIRP-MS. The therapeutic applicability of targeting these lncRNAs with antisense oligonucleotides (ASOs) or small molecule inhibitors warrants systematic evaluation, especially in KRAS/BRAF-mutant CRC models resistant to conventional therapies.

Abbreviations

CRC	Colorectal Cancer
GSEA	Gene Set Enrichment Analysis
FDR	False Discovery Rate
OS	Overall Survival
HRs	Hazard Ratios
CI	Confidence Interval
TCGA	The Cancer Genome Atlas
AUC	Area Under Curve
ROC	Receiver Operating Characteristic
KEGG	Kyoto Encyclopedia of Genes and Genomes

Supplementary Material

The supplementary material can be accessed at https://doi.org/10.11648/j.crj.20251301.12

Acknowledgments

The transcriptome data (HTSeq - FPKM)) and clinical in-

formation were downloaded from The Cancer Genome Atlas (TCGA) (https://cancergenome.nih.gov/). The ferroptosis genes were downloaded from the world's first database of ferroptosis regulators and markers and ferroptosis-disease associations (FerrDb) (http://www.zhounan.org/ferrdb/).

Author Contributions

Yujiao Zhang downloaded the lncRNA and mRNA expression information. Zhiyong Yang constructed the lncRNA signature model and performed the statistical analysis using R language software, and wrote the first draft of the manuscript. Jiping Wang revised the manuscript. Guodong Yang contributed conception and design of the study and checked the manuscript.

Ethics Statement

lncRNA and mRNA sequencing profiles were obtained from the TCGA data portal, which is a publicly available dataset. Therefore, no ethics approval is needed.

Funding

The present study was supported by the Special Scientific Research Fund for Medical Consortium of Hunan Provincial People's Hospital (grant no. 2022YLT005).

Conflicts of Interest

The authors declare that they have no competing interests.

References

[1] Sung H, Ferlay J, Siegel RL, et al. Global Cancer Statistics 2020: GLOBOCAN Estimates of Incidence and Mortality Worldwide for 36 Cancers in 185 Countries. *CA Cancer J Clin*. 2021; 71(3): 209-249. https://doi.org/10.3322/caac.21660

[2] Ferlay J, Steliarova-Foucher E, Lortet-Tieulent J, et al. Cancer incidence and mortality patterns in Europe: estimates for 40 countries in 2012. *Eur J Cancer*. 2013; 49(6): 1374-1403. https://doi.org/10.1016/j.ejca.2012.12.027

[3] Dixon SJ, Lemberg KM, Lamprecht MR, et al. Ferroptosis: an iron-dependent form of nonapoptotic cell death. *Cell*. 2012; 149(5): 1060-1072. https://doi.org/10.1016/j.cell.2012.03.042

[4] Yang WS, SriRamaratnam R, Welsch ME, et al. Regulation of ferroptotic cancer cell death by GPX4. *Cell*. 2014; 156(1-2): 317-331. https://doi.org/10.1016/j.cell.2013.12.010

[5] Li J, Cao F, Yin HL, et al. Ferroptosis: past, present and future. *Cell Death Dis*. 2020; 11(2): 88. Published 2020 Feb 3. https://doi.org/10.1038/s41419-020-2298-2

[6] Fearnhead HO, Vandenabeele P, Vanden Berghe T. How do we fit ferroptosis in the family of regulated cell death?. *Cell Death Differ*. 2017; 24(12): 1991-1998. https://doi.org/10.1038/cdd.2017.149

[7] Sui X, Zhang R, Liu S, et al. RSL3 Drives Ferroptosis Through GPX4 Inactivation and ROS Production in Colorectal Cancer. *Front Pharmacol*. 2018; 9: 1371. Published 2018 Nov 22. https://doi.org/10.3389/fphar.2018.01371

[8] Chen P, Li X, Zhang R, et al. Combinative treatment of β-elemene and cetuximab is sensitive to KRAS mutant colorectal cancer cells by inducing ferroptosis and inhibiting epithelial-mesenchymal transformation. *Theranostics*. 2020; 10(11): 5107-5119. Published 2020 Apr 6. https://doi.org/10.7150/thno.44705

[9] Shen LD, Qi WH, Bai JJ, et al. Resibufogenin inhibited colorectal cancer cell growth and tumorigenesis through triggering ferroptosis and ROS production mediated by GPX4 inactivation [retracted in: Anat Rec (Hoboken). 2021 Dec; 304(12): 2892. https://doi.org/10.1002/ar.24378]. *Anat Rec (Hoboken)*. 2021; 304(2): 313-322.

[10] Sharma P, Shimura T, Banwait JK, Goel A. Andrographis-mediated chemosensitization through activation of ferroptosis and suppression of β-catenin/Wnt-signaling pathways in colorectal cancer. *Carcinogenesis*. 2020; 41(10): 1385-1394. https://doi.org/10.1093/carcin/bgaa090

[11] Park S, Oh J, Kim M, Jin EJ. Bromelain effectively suppresses Kras-mutant colorectal cancer by stimulating ferroptosis. *Anim Cells Syst (Seoul)*. 2018; 22(5): 334-340. Published 2018 Aug 30. https://doi.org/10.1080/19768354.2018.1512521

[12] Zhang L, Liu W, Liu F, et al. Corrigendum to "IMCA Induces Ferroptosis Mediated by SLC7A11 through the AMPK/mTOR Pathway in Colorectal Cancer". *Oxid Med Cell Longev*. 2020; 2020: 6901472. Published 2020 Oct 27. https://doi.org/10.1155/2020/6901472

[13] Xia Y, Liu S, Li C, et al. Discovery of a novel ferroptosis inducer-talaroconvolutin A-killing colorectal cancer cells in vitro and in vivo. *Cell Death Dis*. 2020; 11(11): 988. Published 2020 Nov 17. https://doi.org/10.1038/s41419-020-03194-2

[14] Lu D, Yang Z, Xia Q, et al. ACADSB regulates ferroptosis and affects the migration, invasion, and proliferation of colorectal cancer cells. *Cell Biol Int*. 2020; 44(11): 2334-2343. https://doi.org/10.1002/cbin.11443

[15] Xu X, Zhang X, Wei C, et al. Targeting SLC7A11 specifically suppresses the progression of colorectal cancer stem cells via inducing ferroptosis. *Eur J Pharm Sci*. 2020; 152: 105450. https://doi.org/10.1016/j.ejps.2020.105450

[16] Sun J, Cheng X, Pan S, et al. Dichloroacetate attenuates the stemness of colorectal cancer cells via trigerring ferroptosis through sequestering iron in lysosomes. Environ Toxicol. 2021; 36(4): 520-529. https://doi.org/10.1002/tox.23057

[17] Malfa GA, Tomasello B, Acquaviva R, et al. *Betula etnensis* Raf. (Betulaceae) Extract Induced HO-1 Expression and Ferroptosis Cell Death in Human Colon Cancer Cells. *Int J Mol Sci*. 2019; 20(11): 2723. Published 2019 Jun 3. https://doi.org/10.3390/ijms20112723

[18] Xian ZY, Hu B, Wang T, et al. CircABCB10 silencing inhibits the cell ferroptosis and apoptosis by regulating the miR-326/CCL5 axis in rectal cancer. *Neoplasma*. 2020; 67(5): 1063-1073. https://doi.org/10.4149/neo_2020_191024N1084

[19] Mercer TR, Dinger ME, Mattick JS. Long non-coding RNAs: insights into functions. *Nat Rev Genet*. 2009; 10(3): 155-159. https://doi.org/10.1038/nrg2521

[20] Quinn JJ, Chang HY. Unique features of long non-coding RNA biogenesis and function. *Nat Rev Genet*. 2016; 17(1): 47-62. https://doi.org/10.1038/nrg.2015.10

[21] Mao C, Wang X, Liu Y, et al. A G3BP1-Interacting lncRNA Promotes Ferroptosis and Apoptosis in Cancer via Nuclear Sequestration of p53. *Cancer Res*. 2018; 78(13): 3484-3496. https://doi.org/10.1158/0008-5472.CAN-17-3454

[22] Qi W, Li Z, Xia L, et al. LncRNA GABPB1-AS1 and GABPB1 regulate oxidative stress during erastin-induced ferroptosis in HepG2 hepatocellular carcinoma cells. *Sci Rep*. 2019; 9(1): 16185. Published 2019 Nov 7. https://doi.org/10.1038/s41598-019-52837-8

[23] Wang M, Mao C, Ouyang L, et al. Correction to: Long noncoding RNA LINC00336 inhibits ferroptosis in lung cancer by functioning as a competing endogenous RNA. *Cell Death Differ*. 2020; 27(4): 1447. https://doi.org/10.1038/s41418-019-0394-6

[24] Wang Z, Chen X, Liu N, et al. A Nuclear Long Non-Coding RNA LINC00618 Accelerates Ferroptosis in a Manner Dependent upon Apoptosis. *Mol Ther*. 2021; 29(1): 263-274. https://doi.org/10.1016/j.ymthe.2020.09.024

[25] Gai C, Liu C, Wu X, et al. MT1DP loaded by folate-modified liposomes sensitizes erastin-induced ferroptosis via regulating miR-365a-3p/NRF2 axis in non-small cell lung cancer cells. *Cell Death Dis*. 2020; 11(9): 751. Published 2020 Sep 14. https://doi.org/10.1038/s41419-020-02939-3

[26] Ritchie ME, Phipson B, Wu D, et al. limma powers differential expression analyses for RNA-sequencing and microarray studies. *Nucleic Acids Res*. 2015; 43(7): e47. https://doi.org/10.1093/nar/gkv007

[27] Simon N, Friedman J, Hastie T, Tibshirani R. Regularization Paths for Cox's Proportional Hazards Model via Coordinate Descent. *J Stat Softw*. 2011; 39(5): 1-13. https://doi.org/10.18637/jss.v039.i05

[28] Groeneveld CS, Chagas VS, Jones SJM, et al. RTNsurvival: an R/Bioconductor package for regulatory network survival analysis. *Bioinformatics*. 2019; 35(21): 4488-4489. https://doi.org/10.1093/bioinformatics/btz229

[29] Heagerty PJ, Lumley T, Pepe MS. Time-dependent ROC curves for censored survival data and a diagnostic marker. *Biometrics*. 2000; 56(2): 337-344. https://doi.org/10.1111/j.0006-341x.2000.00337.x

[30] Subramanian A, Tamayo P, Mootha VK, et al. Gene set enrichment analysis: a knowledge-based approach for interpreting genome-wide expression profiles. *Proc Natl Acad Sci U S A*. 2005; 102(43): 15545-15550. https://doi.org/10.1073/pnas.0506580102

[31] Adam R, de Gramont A, Figueras J, et al. Managing synchronous liver metastases from colorectal cancer: a multidisciplinary international consensus. *Cancer Treat Rev*. 2015; 41(9): 729-741. https://doi.org/10.1016/j.ctrv.2015.06.006

[32] Bhan A, Soleimani M, Mandal SS. Long Noncoding RNA and Cancer: A New Paradigm. *Cancer Res*. 2017; 77(15): 3965-3981. https://doi.org/10.1158/0008-5472.CAN-16-2634

[33] Liang JY, Wang DS, Lin HC, et al. A Novel Ferroptosis-related Gene Signature for Overall Survival Prediction in Patients with Hepatocellular Carcinoma. *Int J Biol Sci*. 2020; 16(13): 2430-2441. Published 2020 Jul 6. https://doi.org/10.7150/ijbs.45050

[34] Zhuo S, Chen Z, Yang Y, Zhang J, Tang J, Yang K. Clinical and Biological Significances of a Ferroptosis-Related Gene Signature in Glioma. *Front Oncol*. 2020; 10: 590861. Published 2020 Nov 20. https://doi.org/10.3389/fonc.2020.590861

[35] Yang G, Zhang Y, Yang J. A Five-microRNA Signature as Prognostic Biomarker in Colorectal Cancer by Bioinformatics Analysis. *Front Oncol*. 2019; 9: 1207. Published 2019 Nov 12. https://doi.org/10.3389/fonc.2019.01207

[36] Bai J, Zhang X, Xiang ZX, Zhong PY, Xiong B. Identification of prognostic immune-related signature predicting the overall survival for colorectal cancer. *Eur Rev Med Pharmacol Sci*. 2020; 24(3): 1134-1141. https://doi.org/10.26355/eurrev_202002_20164

[37] Zhang J, Cheng X, Wang J, Huang Y, Yuan J, Guo D. Gene signature and prognostic merit of M6a regulators in colorectal cancer. *Exp Biol Med (Maywood)*. 2020; 245(15): 1344-1354. https://doi.org/10.1177/1535370220936145

[38] Hu X, Li YQ, Ma XJ, Zhang L, Cai SJ, Peng JJ. A Risk Signature With Inflammatory and T Immune Cells Infiltration in Colorectal Cancer Predicting Distant Metastases and Efficiency of Chemotherapy. *Front Oncol*. 2019; 9: 704. Published 2019 Aug 13. https://doi.org/10.3389/fonc.2019.00704

[39] Tokunaga R, Nakagawa S, Sakamoto Y, et al. 12-Chemokine signature, a predictor of tumor recurrence in colorectal cancer. *Int J Cancer*. 2020; 147(2): 532-541. https://doi.org/10.1002/ijc.32982

[40] Zong Z, Li H, Yi C, Ying H, Zhu Z, Wang H. Genome-Wide Profiling of Prognostic Alternative Splicing Signature in Colorectal Cancer. *Front Oncol*. 2018; 8: 537. Published 2018 Nov 20. https://doi.org/10.3389/fonc.2018.00537

[41] Li K, Zeng L, Wei H, et al. Identification of gene-specific DNA methylation signature for Colorectal Cancer. *Cancer Genet*. 2018; 228-229: 5-11. https://doi.org/10.1016/j.cancergen.2018.05.003

[42] Zhou Z, Mo S, Dai W, et al. Development and Validation of an Autophagy Score Signature for the Prediction of Post-operative Survival in Colorectal Cancer. *Front Oncol*. 2019; 9: 878. Published 2019 Sep 9. https://doi.org/10.3389/fonc.2019.00878

[43] Wu B, Tao L, Yang D, Li W, Xu H, He Q. Development of an Immune Infiltration-Related Eight-Gene Prognostic Signature in Colorectal Cancer Microenvironment. *Biomed Res Int*. 2020; 2020: 2719739. Published 2020 Aug 27. https://doi.org/10.1155/2020/2719739

[44] Li Z, Wang D, Yin H. A seven immune-related lncRNA signature predicts the survival of patients with colon adenocarcinoma. *Am J Transl Res*. 2020; 12(11): 7060-7078. Published 2020 Nov 15.

[45] Zhou W, Zhang S, Li HB, et al. Development of Prognostic Indicator Based on Autophagy-Related lncRNA Analysis in Colon Adenocarcinoma. *Biomed Res Int*. 2020; 2020: 9807918. Published 2020 Sep 2. https://doi.org/10.1155/2020/9807918

[46] Jafarzadeh M, Soltani BM, Soleimani M, Hosseinkhani S. Epigenetically silenced LINC02381 functions as a tumor suppressor by regulating PI3K-Akt signaling pathway. *Biochimie*. 2020; 171-172: 63-71. https://doi.org/10.1016/j.biochi.2020.02.009

[47] Jafarzadeh M, Soltani BM. Long Noncoding RNA LOC400043 (LINC02381) Inhibits Gastric Cancer Progression Through Regulating Wnt Signaling Pathway [retracted in: Front Oncol. 2023 Dec 05; 13: 1298859.]. *Front Oncol*. 2020; 10: 562253. Published 2020 Oct 23. https://doi.org/10.3389/fonc.2020.562253

[48] Chen X, Zhang Z, Ma Y, Su H, Xie P, Ran J. LINC02381 Promoted Cell Viability and Migration via Targeting miR-133b in Cervical Cancer Cells. *Cancer Manag Res*. 2020; 12: 3971-3979. Published 2020 May 26. https://doi.org/10.2147/CMAR.S237285

[49] Wei J, Ge X, Tang Y, et al. An Autophagy-Related Long Noncoding RNA Signature Contributes to Poor Prognosis in Colorectal Cancer. *J Oncol*. 2020; 2020: 4728947. Published 2020 Oct 21. https://doi.org/10.1155/2020/4728947

[50] Friedmann Angeli JP, Krysko DV, Conrad M. Ferroptosis at the crossroads of cancer-acquired drug resistance and immune evasion. *Nat Rev Cancer*. 2019; 19(7): 405-414. https://doi.org/10.1038/s41568-019-0149-1

[51] Elgendy SM, Alyammahi SK, Alhamad DW, Abdin SM, Omar HA. Ferroptosis: An emerging approach for targeting cancer stem cells and drug resistance. *Crit Rev Oncol Hematol*. 2020; 155: 103095. https://doi.org/10.1016/j.critrevonc.2020.103095